A Design of Dual-Band Pass Filter for IEEE 802.11 a/b/g Wireless LAN

by Li Rui

Under Supervision of Prof. Dong Il Kim

Department of Radio Sciences and Engineering

in the Graduate School

of the

Korea Maritime University

February 2005

A Design of Dual-Band Pass Filter for IEEE 802.11 a/b/g Wireless LAN

by Li Rui

Here is approved that this is the thesis

submitted in partial satisfaction of the requirements for degree of

MASTER

in Engineering in the Graduate School of the

Korea Maritime University.

Approved : Prof. Kyeong-Sik Min

Prof. In-ho Kang

Prof. Dong Il Kim

Committee in Charge

Contents

Nomenclature

f	:	Frequency
f_0	:	Center frequency
f_n	:	Normalized frequency
FBW	:	Fractional Bandwidth
$S_{ij}(i = j)$	:	Reflection coefficient
$S_{ij}(i \neq j)$	:	Transmission coefficient
Z_0	:	Characteristic Impedance
$[S]$	:	Scattering Matrix
$[T]$	:	Transfer Matrix
Γ_e	:	Reflection coefficient of the even-mode excitation
Γ_o	:	Reflection coefficient of the even-mode excitation
λ	:	Wavelength

List of Tables

List of Fig.s

Abstract

In recent years, dual-band filters have become important components for wireless communication products at microwave frequencies. IEEE 802.11b and IEEE 802.11g wireless local area networks (WLAN) products operate in the unlicensed industrial-scientific-medical (ISM) 2.4- GHz band. In particular, IEEE 802.11a products implement in the ISM 5- GHz band. Therefore, dual-band RF components such as dual-band filters, antenna, and amplifier are essential for the development of mobile communications to design more effective RF devices.

This thesis presents a dual-band pass filter structure which consists of a wide-band pass filter and a band stop filter in a cascade connection. This method has been already proposed in some published paper. In this thesis, the band stop filter is implemented by using a serial-shunted structure, while the wide-band pass filter is constructed by employing three cascade ring resonators. Both two circuits are based on microstrip transmission line structure. In particular, the bandwidth of each pass band of the dual-band filter and the center frequency of the operation band are controllable by adjusting the characteristic impedance of both the wide-band pass filter and the band stop filter. The parameters of the wide-band pass filter are extracted by using Powell's least square method [14] which is a powerful method for calculating the optimum values, and the parameters of the band stop filter are obtained from the Chebyshev low pass prototype.

A dual-band pass filter designed by the method proposed in this thesis has been fabricated and measured. The results agree well with the simulation results. Therefore, it was confirmed that the proposed design method of a dual-band filter for IEEE 802.11a/b/g is available.

요 약

최근에 dual-band 필터는 초고주파수에서 무선 통신 제품을 위해 중요한 소자가 되고 있다. IEEE 802.11b 와 IEEE 802.11g 무선 랜 제품들은 주파수 면허를 받을 필요가 없는 Industrial-Scientific-Medical(ISM) 2.4- GHz 대에서 이용한다. 특히 IEEE 802.11a 무선 랜 제품은 ISM 5- GHz 대를 사용한다. 따라서 더욱 효과적인 RF 장치를 설계하는데 dual-band filter, 안테나, 증폭기와 같은 dual-band RF 소자들은 필수적이고, 그것은 이동통신의 발전에 중요하다.

이 논문은 BPF 와 BSF 가 직렬로 구성되어있는 dual-band 통과필터 구조를 보여준다. 본 논문에서는 BSF 는 serial-shunted 구조를 사용하여 실현하고 광 대역 BPF 는 3 단 링 공진기를 사용해서 만들었다. 두 회로는 마이크로 스트립 전송 선로를 기본으로 한다. 특히, dual-band 필터의 각 통과대역의 대역폭과 동작주파수는 광 대역 BPF 와 BSF 의 특성 임피던스를 조정함으로써 제어할 수 있다. 광 대역 BPF 의 파라미터는 최적 값을 계산할 수 있는 막강한 방법인 Powell's 최소 자승법을 사용해서 구할 수 있다. 그리고, band stop filter 의 파라미터는 고전적인 Chebyshev 저역통과 프로토타입으로부터 얻을 수 있다.

본 논문에서 제안한 방법으로 dual-band pass filter 를 만들고 측정하였다. 측정 결과는 시뮬레이션 결과와 거의 일치했다. 그래서 이 논문에서 dual-band pass filter 설계에 대한 새로운 가능성을 제안한다.

CHAPTER 1 Introduction

The microwave region of the electromagnetic spectrum has certain properties. These enable microwave signals to propagate over long distances through the atmosphere under all but the most severe weather conditions. Both civilian and military applications abound, including radar, navigation, and the latest “hot application,” wireless communications. However, the microwave spectrum is a finite resource which must be divided, cared for, and treated with respect. And this is where microwave filters come in [1]. Emerging applications such as wireless communications continue to challenge RF/microwave filters with ever more stringent requirements such as higher performance, small size, lighter weight, and more important factor-lower cost. The recent advances in novel materials and fabrication technologies, including high-temperature superconductors (HTS), low-temperature cofired ceramics (LTCC), monolithic microwave integrated circuits (MMIC), microelectromechanic system (MEMS), and micromachining technology, have stimulated the rapid development of new microstrip and other filters for RF/Microwave applications [2].

This thesis presents a dual-band pass filter structure which is constructed by employing the microstrip transmission line. Because the microstrip line structure has the advantages of being fabricated easily, lower cost, and the high performances for some RF/Microwave applications.

1.1 Background and Purpose

Present research on microwave filters is very active because of the continuous demands of high-performance circuits from modern communication and electronic system. Most of the work thus far has focused mainly on the filters for a single frequency band, and the filters of multiple frequency bands have been largely ignored. In recent years, dual-band filters have become important components for wireless communication products at microwave frequencies. For example, global systems for mobile communications (GSM) operate at both 900 and 1800 MHz. IEEE 802.11b [3]-[4] and IEEE 802.11g [4]-[5] wireless local area networks (WLANs) products operate in the unlicensed industrial-scientific-medical (ISM) 2.4- GHz band. In particular, IEEE 802.11a [6] products implements in the ISM 5- GHz band [7]. Therefore, dual-band RF components such as dual-band filters, antenna and amplifier are essential for the development of mobile communications to design some more effective and backward compatible RF devices.

In this thesis, a new configuration of dual-band pass filter which can cover the two ISM bands 2.4- GHz and 5- GHz is proposed. The dual-band pass filter consists of a wide-band pass filter and a band stop filter in a cascade connection.

1.2 Research Contents

Chapter 1 depicts the background and purpose of this work and

briefly introduces the outline of the thesis.

Chapter 2 focus on a design of wide-band pass filter. The theoretical analysis, circuit design and the simulated results by ADS (Advanced Design System) are presented in this chapter.

Chapter 3 introduces some types of the band stop filters based on microstrip line structure briefly. And in addition, the theoretical analysis and design method are explained in detail here.

Chapter 4 shows how the dual-band pass filter is realized by using the wide-band filter and band stop filter as presented in previous chapters. And the evaluation for this design proposed in this thesis is exhibited in this chapter.

Chapter 5 is the conclusion of this research work and presents a future plan.

CHAPTER 2 **Wide-band Pass Filter**

2.1 Introduction

It is well-known that there are four types of filters in RF/Microwave system mainly, such as Low Pass Filter, High Pass Filter, Band Pass Filter, and Band Stop Filter. In this chapter, we will present a design of wide-band filter based on microstrip transmission line structure.

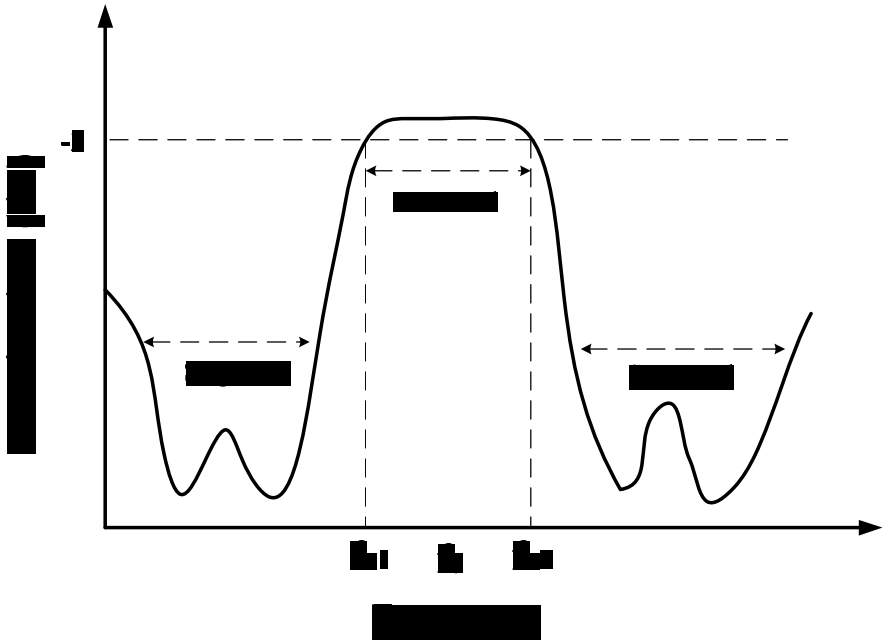

Fig. 2.1 Frequency responses of a band pass filter

A band pass filter is an electronic device or circuit that allows signals between two specific frequencies to pass, but that

discriminates against signals at other frequencies. It is used extensively in mobile communications system, especially, used in communication receivers and transmitters, primarily.

Fig. 1 illustrates the typical frequency responses of a band pass filter. The cutoff frequencies, $\mathbf{f}_{c1}$ and $\mathbf{f}_{c2,}$ are the frequencies at which the output signal power falls to half of its level at $\mathbf{f}_0$, the center frequency of the filter. The value $\mathbf{f}_{c1}$ - $\mathbf{f}_{c2,}$ expressed in hertz (Hz), kilohertz (KHz), megahertz (MHz), or gigahertz (GHz), is called the filter bandwidth. The range of frequencies between $\mathbf{f}_{c1}$ and $\mathbf{f}_{c2}$ is called the filter pass band [8].

There are many types of BPFs (Band Pass Filters) such as end-coupled, half-wavelength resonator filters, parallel-coupled, half-wavelength resonator filters, hairpin-line filters and inter-digital band-pass filters, etc. In this thesis, however, we decide to design the wide-band BPF by employing cascade ring resonators. The reasons why we do not use the others are explained below. One reason is that we need a wide-band pass filter from 2.35 GHz-5.05 GHz, but just the parallel-coupled, half-wavelength resonator, series-shunted transmission line structure and ring resonator can achieve the bandwidth we need. Nevertheless, if we implement the wide-band pass filter with the bandwidth we need by employing series-shunted transmission line structure, the wide-BPF size should be larger than by using the ring resonator structure [2], and further more, the ring-filter is more easier to fabricate than the coupled-line structure BPF. It is more important just that the BPF with ring resonator has more high performance,

lower insertion loss and better skirt characteristics [9]-[11].

2.2 Theoretical Analysis

The schematic diagram of a three-stage ring resonator filter is shown in Fig. 2.2.

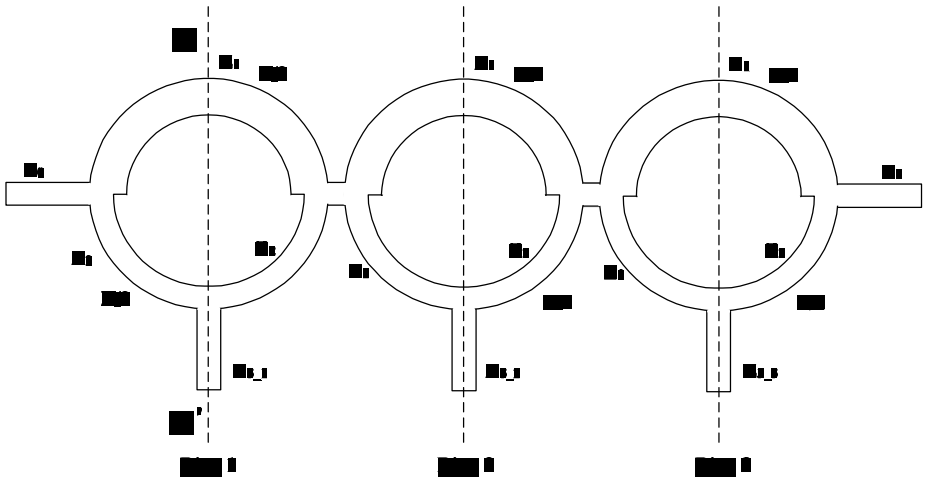

Fig. 2.2 Schematic diagram of a three-stage ring resonator filter

As shown in Fig. 2.2, the total length of the ring is chosen to be equal to one wavelength at the center frequency. The ring has characteristic impedances of Z_1 and Z_2 and a length of λ. Three open stubs have their length of $\lambda/4$ and characteristic impedance of Z_{3_1}, Z_{3_2} and Z_{3_3}, respectively.

One stage ring filter will be analyzed firstly, and its results will be applied to the three-stage ring filter.

2.2.1 Even-mode Analysis

From Fig. 2.2, we can find that the each separate ring resonator circuit is symmetrical and reciprocal along the AA' axis, and therefore we can analyze this circuit by the even-odd mode method.

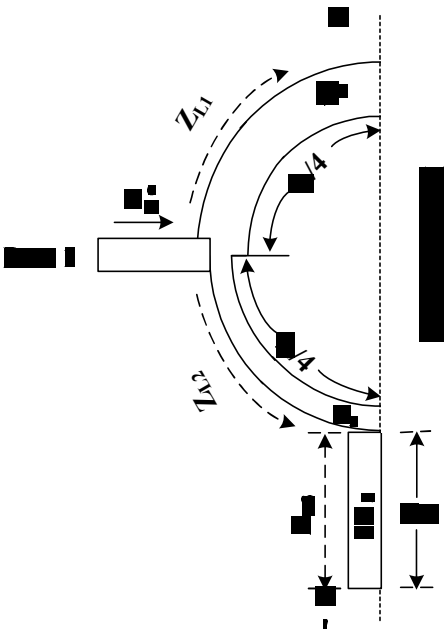

Fig. 2.3 Even-mode equivalent circuit

The even mode excitation is obtained by applying equal waves at two ports of the network, while the odd mode excitation is obtained by applying out-of-phase waves at ports 1 and 2. Equivalent circuits for these two modes are shown in Fig. 2.3 and Fig. 2.4 [13] in which Z_{L1} and Z_{L2} are the input impedances for even-mode and odd-mode, respectively.

The input impedance Z_{in}^{e} for even-mode, which is illustrated in Fig. 2.3, can be calculated by using the well-known transmission line theory [8]. Since Z_{L1} is input impedance with an open stub, so it is expressed as equation (2.1) below.

$$Z_{L1} = -jZ_1 \cot(\frac{\pi}{2} \cdot f_n) \tag{2.1}$$

Where Z_{L1} and Z_1 are input and characteristic impedance shown in Fig. 2.3 and f_n is a normalized frequency by center frequency f_0, and expressed as equation (2.2).

$$f_n = \frac{f}{f_0} \tag{2.2}$$

The input impedance of the open-stub employed in ring resonator circuit is calculated as equation (2.3).

$$Z_{L3} = -j2Z_3 \cot(\frac{\pi}{2} \cdot f_n) \tag{2.3}$$

And then we can calculated Z_{L2} using this obtained result above.

$$Z_{L2} = Z_2 \frac{Z_{L3} + jZ_2 \tan(\frac{\pi}{2} \cdot f_n)}{Z_2 + jZ_{L3} \tan(\frac{\pi}{2} \cdot f_n)} \tag{2.4}$$

Where Z_{L3} and Z_3 are the input and stub characteristic impedances shown in Fig. 2.3. Even-mode input impedance Z_{in}^{e} can be expressed as equation (2.5).

$$Z_{in}^{e} = \frac{Z_{L1} \cdot Z_{L2}}{Z_{L1} + Z_{L2}} \tag{2.5}$$

Therefore, the even-mode reflection coefficient can be derived as follows.

$$\Gamma_e = \frac{Z_{in}^{e} - Z_0}{Z_{in}^{e} + Z_0} \tag{2.6}$$

2.2.2 Odd-mode Analysis

Odd-mode equivalent circuit is shown in Fig. 2.4.

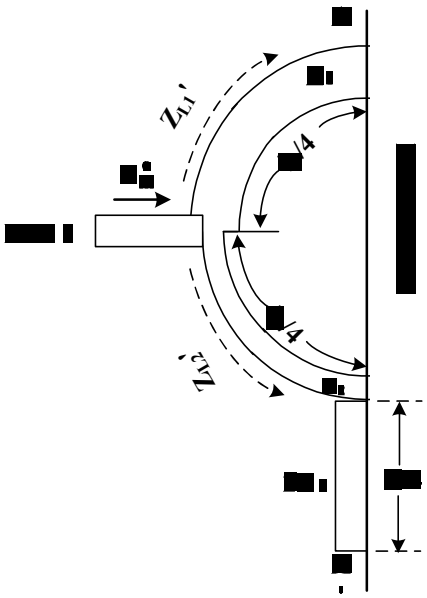

Fig. 2.4 Odd-mode equivalent circuit

All the parameters $Z_{L1}^{'}, Z_{L2}^{'}, Z_{in}^{o}$, etc. in the odd-mode equivalent circuit can be calculated in the same manner as the one used for the

even-mode analysis. In this case, the odd-mode reflection coefficient is shown as follows.

$$\Gamma_0 = \frac{Z_{in}^o - Z_0}{Z_{in}^o + Z_0} \tag{2.7}$$

2.2.3 S-parameter Extraction from Even-odd Mode.

The scattering parameters of each ring resonator circuit are extracted by the above results from even-odd mode analysis.

$$S_{11} = \frac{\Gamma_e + \Gamma_e}{2} \tag{2.8}$$

$$S_{21} = \frac{\Gamma_e - \Gamma_e}{2} \tag{2.9}$$

According to the symmetrical and reciprocal properties, S_{12} and S_{22} can be obtained from equation (2.8) and (2.9) directly as follows:

$$S_{22} = S_{11} \tag{2.10}$$

$$S_{12} = S_{21} \tag{2.11}$$

2.2.4 Analysis of 3-Stage Ring Resonators Circuit.

Fig. 1 shows a 3-stage ring filter. The analysis method for ring 2

and ring 3 is the same with that for ring 1. In order to calculate the reflection coefficients of this cascade circuit simply, the transfer matrices is necessary [9]. The calculation processes are explained as follows. First, the transfer matrix of the single ring filter shown in should be calculated.

$$T_i = \begin{bmatrix} T_{11}^i & T_{12}^i \\ T_{21}^i & T_{22}^i \end{bmatrix} \tag{2.12}$$

Where

$$T_{12}^i = S_{12}^i - \frac{S_{11}^i \cdot S_{22}^i}{S_{21}^i}$$

$$T_{12}^i = \frac{S_{11}^i}{S_{21}^i}$$

$$T_{21}^i = -\frac{S_{22}^i}{S_{21}^i}$$

$$T_{22}^i = \frac{1}{S_{21}^i} \tag{2.13}$$

Then the cascade transfer matrix of the total circuit is

$$[T_t] = [T_1] \cdot [T_2] \cdot [T_3] \tag{2.14}$$

2.3 A design of 2.35-5.05 GHz Band Pass Filter.

For the purpose of this work, we should design a wide-band pass filter whose bandwidth is from 2.35 GHz to 5.05 GHz. Based on the

analysis presented in the previous section, the design method and processes for this circuit are demonstrated below

Above all, a calculation method of Powell's Least Square Method [12] is introduced simply now. Powell's Least Square Method is a powerful method for minimizing a sum of squares of non-linear parity functions without derivatives. There are a number of approaches to optimizing an objective function. When one is able to graph a function and look at it, it is very easy to discover the minimum point in that function. However, in complex analysis such a visual aid is impossible to produce without enormous expenditures of time and computing resources. Every time a function is evaluated, it is costing somebody money. In a business setting, therefore, the number of function calls must be decreased when optimizing a function or design space. There are a number of algorithms that can accomplish this. The purpose of the program described herein is to optimize a function consisting of at most 10 independent variables by finding its minimum value. The manner in which this is accomplished is by using Powell's Method to define a search direction, and a quadratic line search to find the minimum point along that search direction. After a certain number of Powell iterations, line searches, and function calls, a reasonable minimum can usually be produced, if not completely exact.
The parity functions used in this paper are shown below:

Within the pass band spectra:

$f_1 = 2.35 \sim 5.05 \quad GHz$

$$F_1(Z_1, Z_2, Z_3, Z_4, Z_5, f_1) = \sum \left(|S_{11}|^2 + (1 - |S_{21}|)^2 \right) \quad (2.15)$$

Within the first stop band spectra:

$$f_2 = 1.35 \sim 2.35 \quad GHz$$
$$F_2(Z_1, Z_2, Z_3, Z_4, Z_5, f_2) = \sum \left(|S_{21}|^2 + (1 - |S_{11}|)^2 \right) \quad (2.16)$$

Within the second stop band spectra:

$$f_3 = 5.05 \sim 6.05 \quad GHz$$
$$F_3(Z_1, Z_2, Z_3, Z_4, Z_5, f_3) = \sum \left(|S_{21}|^2 + (1 - |S_{11}|)^2 \right) \quad (2.17)$$

Therefore, the total parity function is

$$F_t = F_1 + F_2 + F_3 \quad (2.18)$$

A search cycle of this method starts with the conventional ring resonators circuit parameters shown in [10], and the obtained optimal results are shown in Table 1 below.

Table 2.1 Parameters extracted by Powell's Least Square Method.

Z_1	Z_2	Z_{3-1}	Z_{3-2}	Z_{3-3}
55 Ω	120 Ω	16 Ω	25 Ω	40 Ω

2.4 Simulation Results.

The theoretical frequency responses are shown in Fig. 2.5 below.

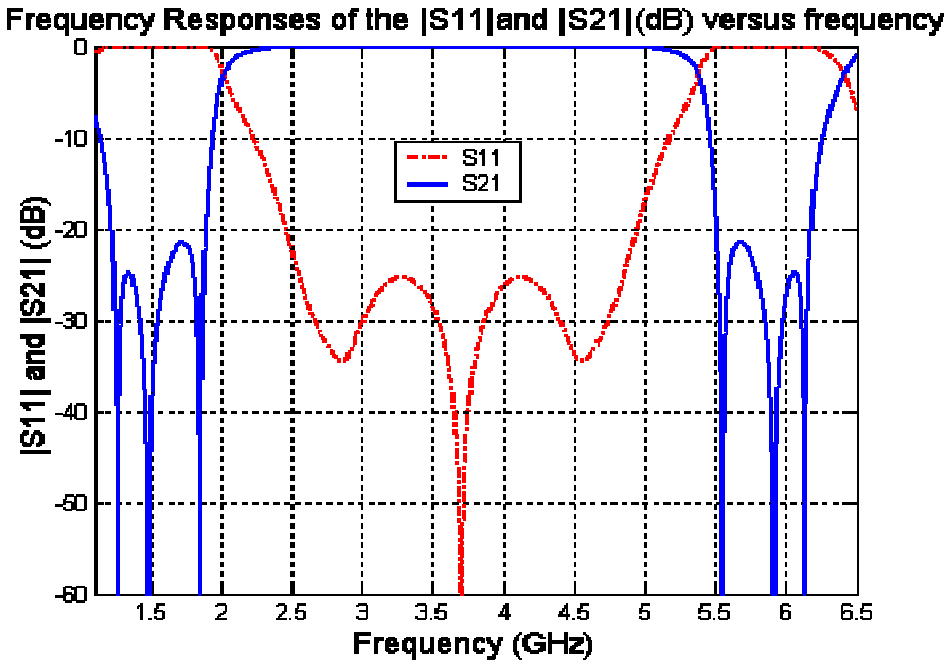

Fig. 2.5 Theoretical Frequency Responses

As shown in above Fig., the pass band is from 2.35~5.05 GHz, and the out of pass band, i.e. two stop bands have become less than -20 dB.

And now the simulation results by using ADS (Advanced Design Simulation) tool are exhibited below, and compared with the theoretical results.

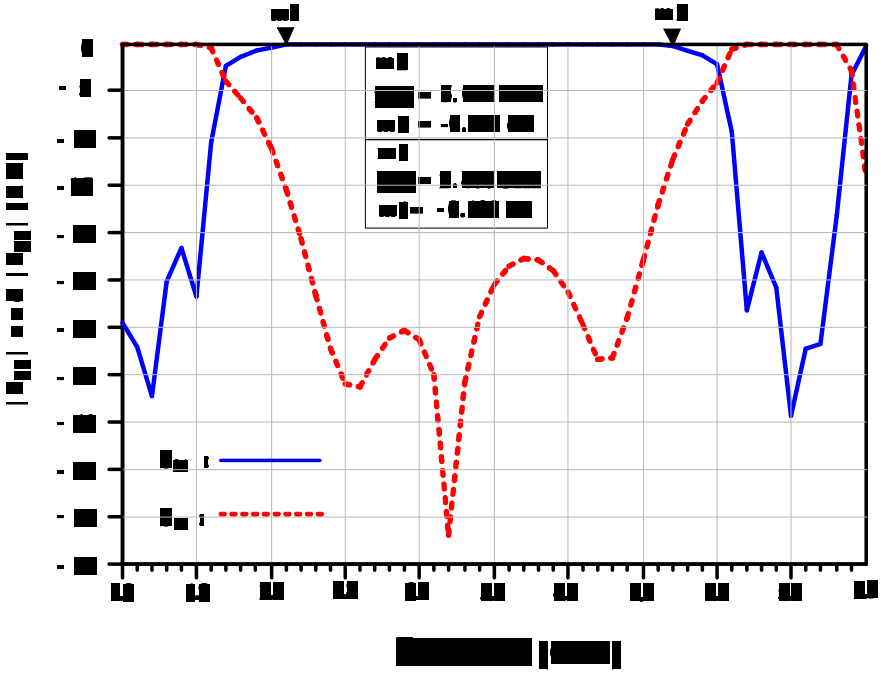

Fig. 2.6 Simulation results by ADS.

Comparing the simulation results with the theoretical results, we can find that our design scheme is reasonable and practicable.

The physical sizes of this wide-band pass filter proposed in this thesis are shown in Table 2 below.

Table 2.2 Physical sizes of this wide-band pass filter.

Z_0 (Ω)	Width (mm)	1.0909
50	Length(mm)	12.2833
Z_1(Ω)	Width (mm)	0.9283
55	Length(mm)	24.7457
Z_2(Ω)	Width (mm)	0.1355
120	Length(mm)	26.4401
$Z_{3\text{-}1}$(Ω)	Width (mm)	5.1422
16	Length(mm)	11.4567
$Z_{3\text{-}2}$(Ω)	Width (mm)	3.1218
24	Length(mm)	11.6994
$Z_{3\text{-}1}$(Ω)	Width (mm)	1.2926
45	Length(mm)	12.1880

Printed Circuit Board: Metal thickness: 0.034mm.
Substrate thickness: 0.5mm.
Relative permittivity: 3.5.

CHAPTER 3 **Band Stop Filter**

3.1 Introduction

As presented in chapter 2, we know that band stop filters are also very important components in RF/Microwave system, and its frequency responses are shown in Fig. 3.1. The features of band stop filters can be understood easily with reference to the relational description in chapter 2.

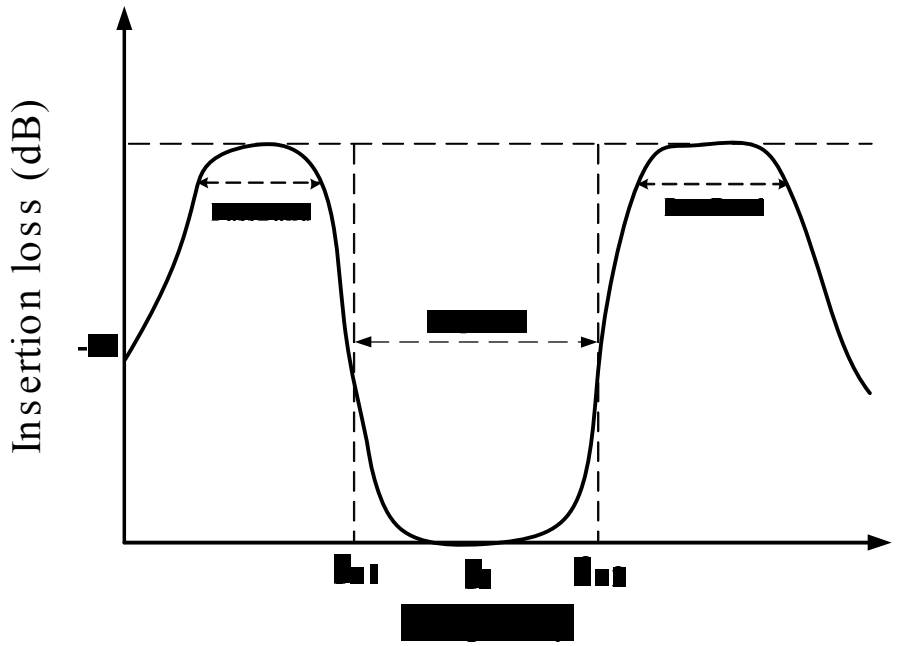

Fig. 3.1 Typical frequency responses of a band stop filter

Where do we apply band stop filters usually? When the rejection of a signal is required, it is natural to think in terms of a notch. Just as

a true band pass filter offers improved selectivity over a single resonator, the band stop filter offers improved rejection over a simple notch or even a cascade of notches. However, the general realization difficulties of distributed structures are worsened by particular difficulties associated with the band stop structure.

In this thesis, we intend to design a band stop filter with microstip line structure. A schematic diagram is shown in Fig. 3.2 below.

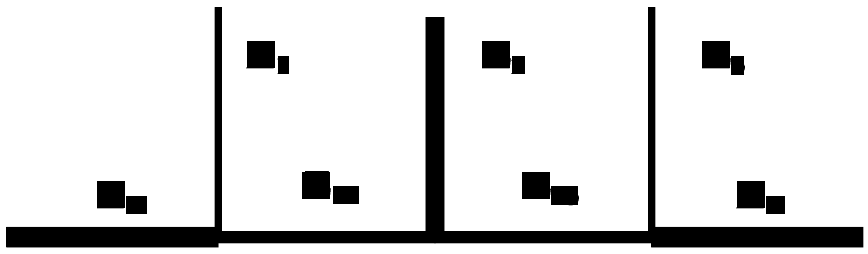

Fig. 3.2 Schematic diagram of band stop filter with serial-shunted subs for $n = 3$

Fig. 3.2 is a transmission line structure of a band stop filter with three open-circuit-shunted stubs (n=3), where the shunt quarter-wavelength, open-circuited stubs are separated by unit elements (connecting lines) that are a quarter wavelength long at the mid-stop-band frequency. Filtering characteristics of the filter then entirely depends on design of characteristic impedances Z_i for the open-circuited stubs, and characteristic impedances $Z_{i,i+1}$ for the unit elements, as well as two terminating impedances Z_A and Z_B ,

respectively, and the other parameters are indicated in corresponding place in Fig. 3.2.

This distributed band stop structures can theoretically be transformed directly from a conventional L-C band stop filter. However, in practice, this direct transformation gives unrealistic line impedances, often on the order of hundreds of ohms. Kuroda's identities [15] can be used to help this process, inserting admittance inverters and forcing the line impedances to become somewhat more reasonable. An edge coupled band stop filter is also available, but is only realizable for very narrow bandwidths. So we propose a band stop filter using the serial–shunted structure, because we must have got a bandwidth of 2.45 GHz ~ 4.95 GHz.

3.2 Theoretical Analysis

Firstly, the theory background is explained below, and a group of optimum formulas will be introduced in section 2.

3.2.1 Theory Background

This band stop filter is designed using a design procedure as described in [16]-[17].

The design procedure starts with a chosen ladder-type low pass prototype. Then it uses a frequency mapping as follows:

$$\Omega = \Omega_c \alpha \tan\left(\frac{\pi}{2}\frac{f}{f_0}\right) \tag{3.1}$$

$$\alpha = \cot\left[\frac{\pi}{2}\left(1-\frac{FBW}{2}\right)\right] \tag{3.2}$$

where Ω and Ω_c are the normalized frequency variable and the cutoff frequency of a low pass prototype filter, f and f_0 are the frequency variable and the mid-band frequency of the corresponding band stop filter, and *FBW* is the fractional bandwidth of the band stop filter defined by

$$FBW = \frac{f_{c2} - f_{c1}}{f_0}$$

$$f_0 = \frac{f_{c1} + f_{c2}}{2} \tag{3.3}$$

f_{c1} and f_{c2} are frequency points in the band stop response as indicated in Fig. 3.1. It should be mentioned that band stop filters of this type have spurious stop bands periodically centered at frequencies that are odd multiples of f_0. At these frequencies, the shunt open-circuited stubs in the filters are odd multiples of $\lambda_{g0}/4$ long, with λ_{g0} being the guided wavelength at frequency f_0, so that they short out the main line and cause spurious stop bands. In this case, there is no need to be concerned about this point because the spurious frequencies are not in the spectral band which we need.

Note that the frequency mapping in equation (3.3) actually involves

the Richards' transformation which demonstrated in Fig. 3.3 below. Therefore, under the mapping of equation (3.3), the shunt (capacitive) elements of low pass prototype become shunt (open-circuited) stubs of the mapped band stop filter, whereas the series (inductive) elements become series (short-circuited) stubs. The series short-circuited stubs are then removed by utilizing Kuroda's identities which are shown in Fig. 3.4 and we can obtain the desired transmission line band stop filter shown as Fig. 3.2 [2].

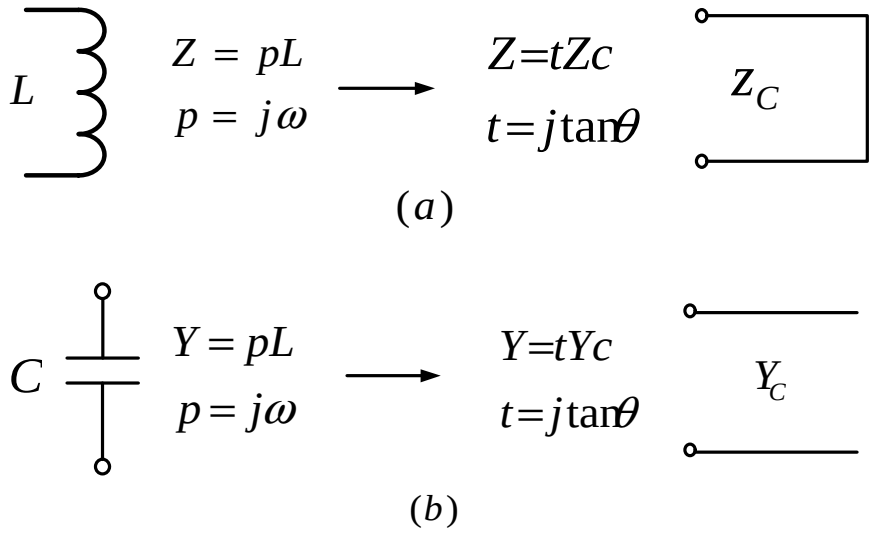

Fig. 3.3 Lumped and distributed element correspondence under Richards' transformation

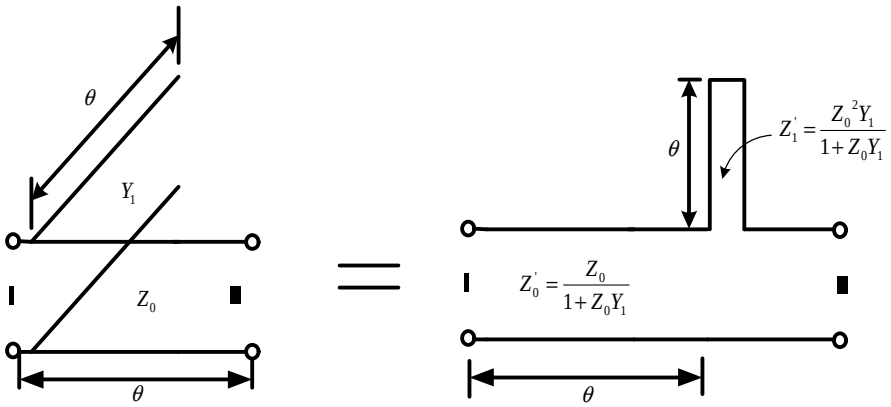

(a)

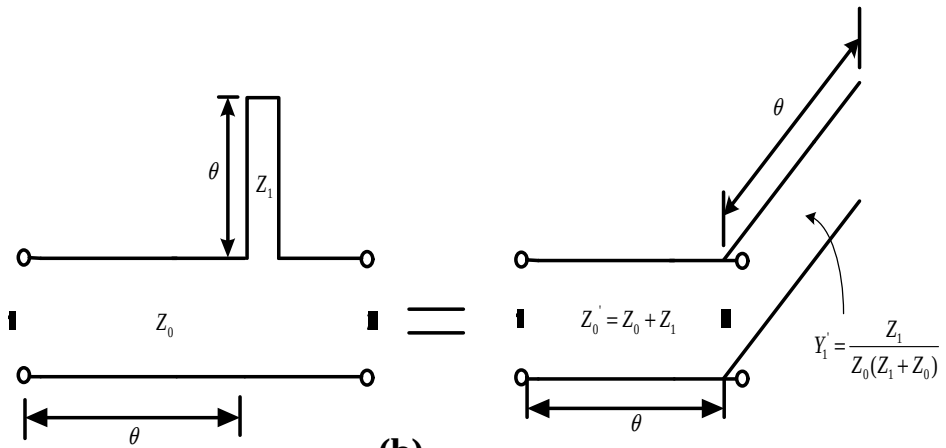

(b)

Fig. 3.4 Kuroda's identity in transmission line form

3.2.2 Optimum Formulas

With the design procedure in the previous section, the unit elements of the band-stop filter are redundant, and their filtering properties are not utilized, so that in this sense, the resultant band stop filter is not an optimum one. It has been pointed out in [17]-[18] that for wide-band band stop filters. The unit elements can be made nearly as effective as the open-circuited stubs. Therefore, by incorporating the unit elements in the design, significantly steeper attenuation characteristics can be obtained for the same number of stubs than is possible for filters designed with redundant unit elements. Also, a specified filter characteristic can be met with a more compact configuration using fewer stubs if the filter is designed by an optimum method.

The optimum formulas are shown below [2].

$$Z_A = Z_B = Z_0$$

$$Z_i = Z_0 / g_i$$

$$Z_{i,i+1} = Z_0 / J_{i,i+1} \qquad (3.4)$$

Where g_i and $J_{i,i+1}$ are the relational optimum parameters, and Z_A, Z_B are the input and output impedances, Z_i is the impedance of open-shunted stubs.

3.3 A design of 2.45~4.95 GHz Band Stop Filter

For the realization of dual-band pass filter, we need a band stop filter with bandwidth of 2.45 ~ 4.95 GHz. So we can obtain the center frequency and FBW (Fractional Bandwidth) from equation (3.3).

$$FBW = \frac{f_{c2} - f_{c1}}{f_0} = 0.702 \quad \text{with} \quad f_0 = \frac{f_{c1} + f_{c2}}{2} = 3.7 \ GHz$$

And that we want to have the circuit size smaller as possible as it can be, so the structures with three open-shunted stubs are employed in this thesis.

For convenience, element values of the network in Fig. 3.2, for design of optimum band stop filters with three open-shunted stubs and a pass band return loss level of -20 dB, are tabulated in Table 3.1 for bandwidths between 30% and 150%. Note that the tabulated elements are the normalized admittances, and for a given reference impedance Z_0 the impedances are determined by equation (3.4).

Table 3.1 Element values of optimum band stop filters for n = 3 and $\varepsilon = 0.1005$

FBW	$g_1 = g_3$	g_2	$J_{1,2} = J_{2,3}$
0.3	0.16318	0.26768	0.97734
0.4	0.23016	0.38061	0.92975
0.5	0.37754	0.63292	0.83956
0.6	0.46895	0.79494	0.78565
0.7	0.56896	0.97488	0.73139
0.8	0.67986	1.17702	0.67677
0.9	0.80477	1.40708	0.62180
1.0	0.94806	1.67311	0.56648
1.1	1.11601	1.98667	0.51082
1.2	1.15215	2.06604	0.49407
1.3	1.37952	2.49473	0.43430
1.4	1.67476	3.05136	0.37349
1.5	2.07059	3.79862	0.31262

In this thesis, we design an optimum microstrip band stop filter with three open-circuited stubs (n=3) and a fractional bandwidth FBW = 0.7 at a midband frequency f_0 = 3.7 GHz will be designed. Assume a pass band loss of -20 dB, which corresponds to a ripple constant $\varepsilon = 0.1005$. From Table 3.1, we obtain the normalized element values $g_1 = g_3 = 0.56896$, $g_2 = 0.97488$ and $J_{1,2} = J_{2,3} = 0.73139$ denoted as highlight area**.** The filter is designed to match 50 ohm terminations. Therefore, Z_0 = 50 ohms, and from equation (3.4) we determine the electrical design parameters for the

filter network representation in Fig. 3.2.

$$Z_A = Z_B = 50\ Ohm$$

$$Z_1 = Z_3 = 87.8796\ \text{Ohm}$$

$$Z_2 = 51.2884 Ohm$$

$$Z_{12} = Z_{23} = 68.3630\ \text{O}hm \qquad (3.4)$$

So far, the circuit designs are accomplished, and the simulation is implemented and the results are shown in next section.

3.4 Simulation.

In this case, we employed the same PCB with the one used for wide-band pass filter design in previous chapter.

The results obtained by using ADS software tool are presented in Fig. 3.5.

Table 3.2 Physical sizes of the band stop filter

Z_A (Ω) 50	Width (mm)	1.0909
Z_B (Ω) 50	Width (mm)	1.0909
Z_1(Ω) 87.8796	Width (mm)	0.3518
	Length(mm)	12.8576
Z_2(Ω) 51.2884	Width (mm)	1.0458
	Length(mm)	12.3069
Z_3(Ω) 87.8796	Width (mm)	0.3518
	Length(mm)	12.8576

Printed Circuit Board: Metal thickness: 0.034mm

Substrate thickness: 0.5mm

Relative permittivity: 3.5

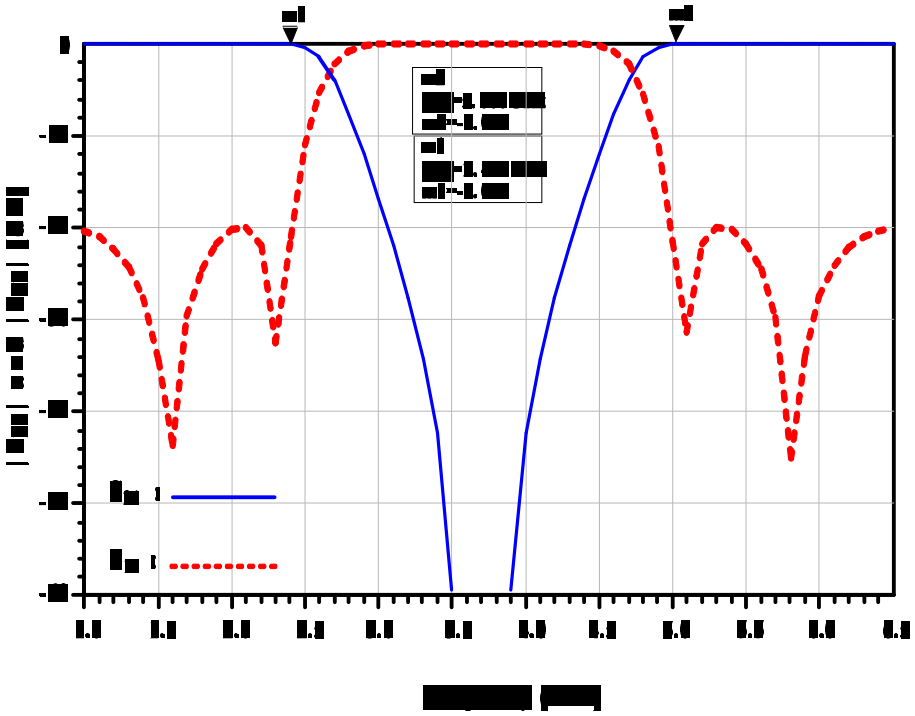

Fig. 3.5 Simulation results by ADS

From Fig. 3.5, the simulation results meet the ideal design purposes well.

CHAPTER 4 Dual-Band Pass Filter

4.1 Theoretical Analysis

In this thesis, we need a cascade circuit constructed with two circuit networks of a wide-band pass filter circuit and a band stop filter circuit shown in Fig. 4.1 below..

Firstly, we should analyze the cascade circuit, and obtain the total s-parameters.

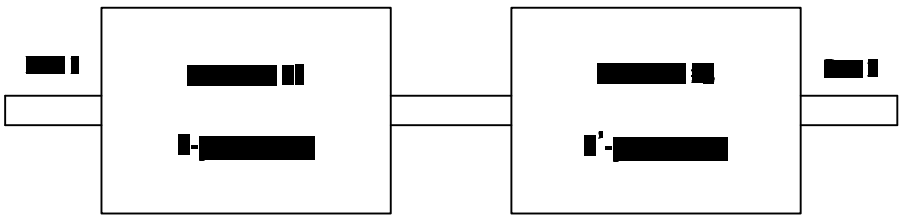

Fig. 4.1 S-parameters of a cascade circuit with two networks

Assumption that the network 1# and 2# have S-parameters and S'-parameters, respectively, and then calculate the S_t-parameters (Total s-parameters) utilizing T – matrices. The analysis procedures are shown below.

For network 1 #:

$$[T_1] = \begin{bmatrix} T_{11} & T_{12} \\ T_{21} & T_{22} \end{bmatrix}$$

Where

$$T_{11} = S_{12} - \frac{S_{11} \cdot S_{22}}{S_{21}}$$

$$T_{12} = \frac{S_{11}}{S_{21}}$$

$$T_{21} = -\frac{S_{22}}{S_{21}}$$

$$T_{22} = \frac{1}{S_{21}} \qquad (4.1)$$

For network 2 #:

$$[T_2] = \begin{bmatrix} T_{11}' & T_{12}' \\ T_{21}' & T_{22}' \end{bmatrix}$$

Where

$$T_{11}' = S_{12}' - \frac{S_{11}' \cdot S_{22}'}{S_{21}'}$$

$$T_{12}' = \frac{S_{11}'}{S_{21}'}$$

$$T_{21}' = -\frac{S_{22}'}{S_{21}'}$$

$$T_{22}' = \frac{1}{S_{21}'} \qquad (4.2)$$

From

$$[T_t] = [T_1] \cdot [T_2] \qquad (4.3)$$

We can obtain the total Transfer matrix $[T_t]$:

$$[T_t] = \begin{bmatrix} T_{11}^t & T_{12}^t \\ T_{21}^t & T_{22}^t \end{bmatrix} \tag{4.4}$$

and

$$[S_t] = \begin{bmatrix} S_{11}^t & S_{12}^t \\ S_{21}^t & S_{22}^t \end{bmatrix}$$

where

$$S_{11}^t = \frac{T_{12}^{\ t}}{T_{22}^{\ t}} \quad , \quad S_{12}^t = T_{11}^t - \frac{T_{12}^{\ t} \cdot T_{21}^{\ t}}{T_{22}^{\ t}} \quad , \; S_{21}^t = \frac{1}{T_{22}^{\ t}} \; , \quad S_{22}^t = -\frac{T_{21}^{\ t}}{T_{22}^{\ t}}$$

So we can deduce the total transmission parameter S_{21}^t from equation (4.1) ~ (4.3).

$$S_{21}^t = \frac{S_{21} \cdot S_{21}^{'}}{1 - S_{22} \cdot S_{11}^{'}} \tag{4.5}$$

For a small value of S_{22} and $S_{11}^{'}$, $S_{21}^{'}$ equals approximately $S_{21} \cdot S_{21}^{'}$. From Fig. 2.6 and 3.5, which represent the simulation results of wide-band pass filter and band stop filter, we can observe that S_{22} and $S_{11}^{'}$ are very small at 2.4 GHz and 5.0 GHz, so the total transmission coefficient $S_{21}^t \approx S_{21} \cdot S_{21}^{'}$. As a result, a dual-band filter can be obtained by a cascade connection of a wide-band pass filter and a band stop filter and its transfer function can be approximated as the product of the transmission coefficients of two filters, S_{21}^{BPF} and S_{21}^{BSF}.

Of course, if network 1# and 2# can not meet the condition, which

S_{22} and $S_{11}^{'}$ are very small values, the cascade circuits should be re-optimized to satisfy the demands we need.

4.2 A design of the Dual-Band Pass Filter and Simulation Results

Fig. 4.2 shows the schematic diagram of the dual-band filter consisted of the wide-band filter and band stop filter discussed in previous two chapters.

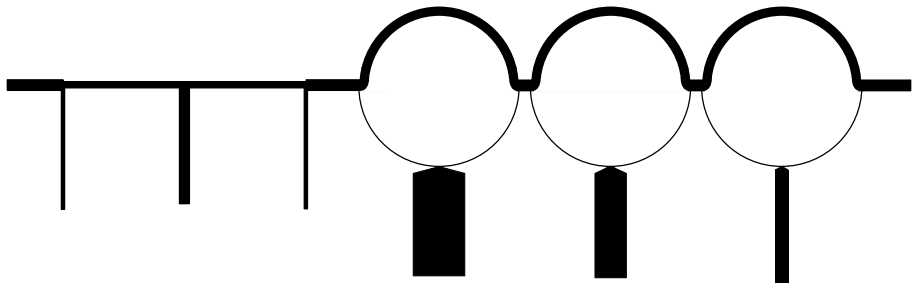

Fig. 4.2 Schematic diagram of a dual-band pass filter

Fig. 4.3 shows the simulation results obtained by ADS.

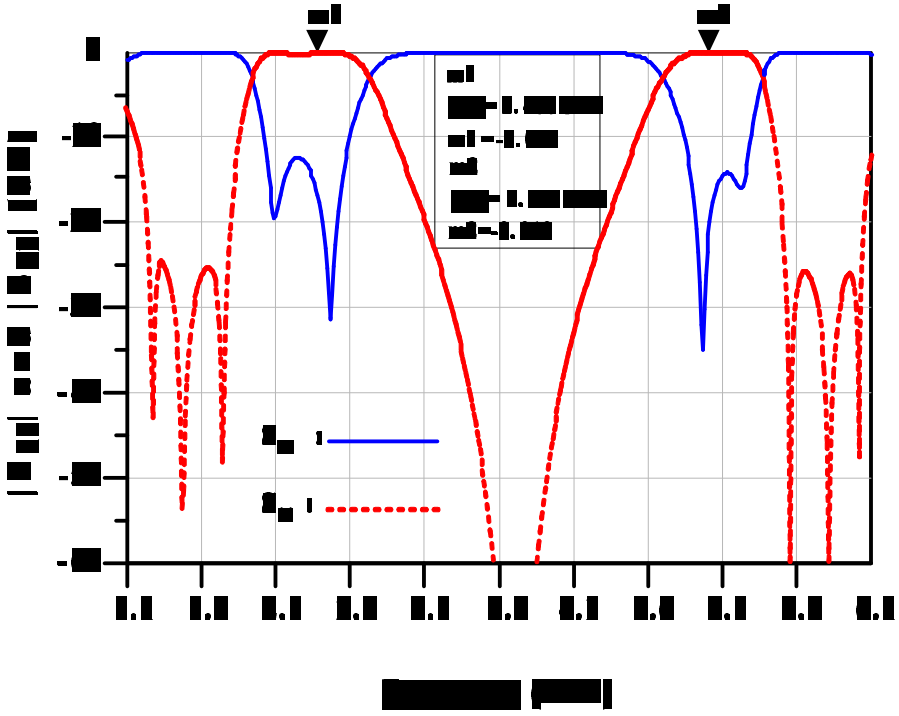

Fig. 4.3 Simulation results of the dual-band pass filter

The physical sizes of this circuit are same as ones described in Table 2.1 and 3.2.

Excluding the reflection coefficient S_{11} and transmission coefficient S_{21}, there is other important coefficient which is called as group delay. It is one of the main factors that can influence the performances of the filters. The simulation result of group delay is shown in Fig. 4.4.

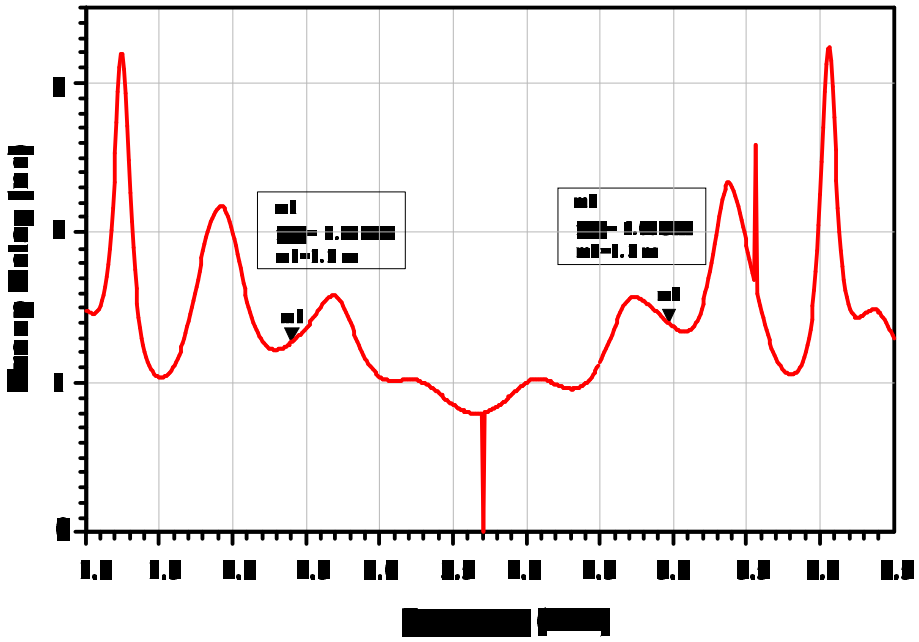

Fig. 4.4 Simulation result of Group Delay

Fig. 4.4 indicates that the GD (Group Delay) values are 1.2~1.3 ns and 1.3~1.4 ns within two bands centered at 2.4 GHz and 5.0 GHz, respectively. It shows a good flatting characteristic.

4.3 Fabrication and Measurement.

A photograph of the dual-band pass filter proposed in this thesis is shown below.

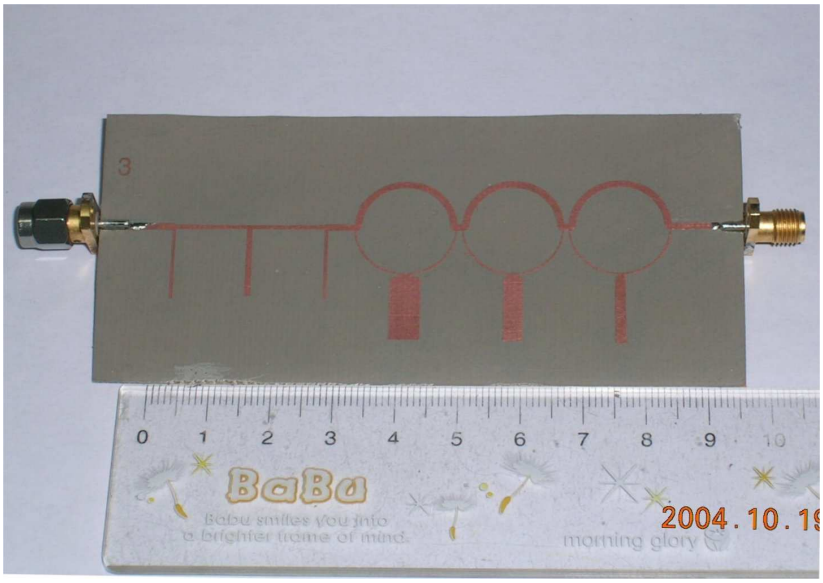

Fig. 4.5 Photograph of the dual-band pass filter proposed in this thesis

The total length of the filter excluding 50Ω reference lines on both sides is 85 mm. It is proved that this cascade circuit is smaller than the other one fabricated by different cascade structure proposed in [7].

Fig. 4.6 shows that the measured results by Wiltron Network Analyzer 360B and HP 8753D.

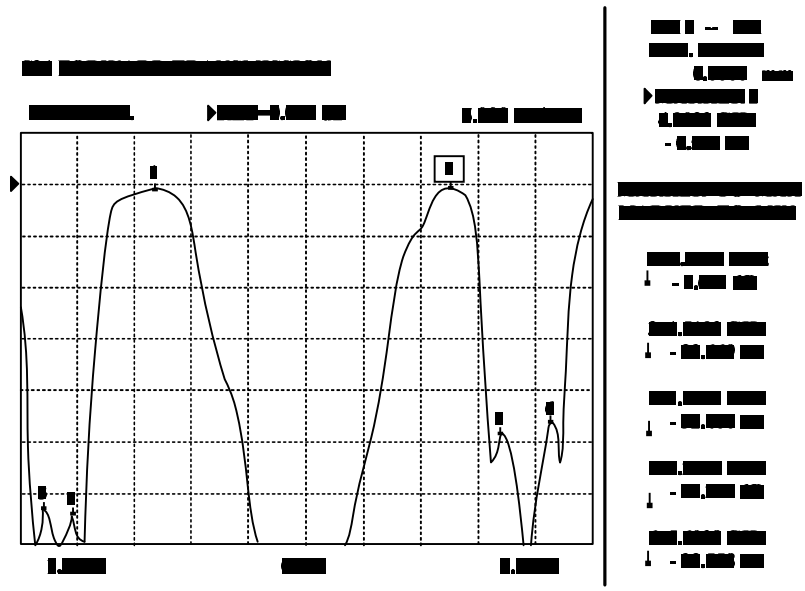

(a) Transmission coefficient S_{21}

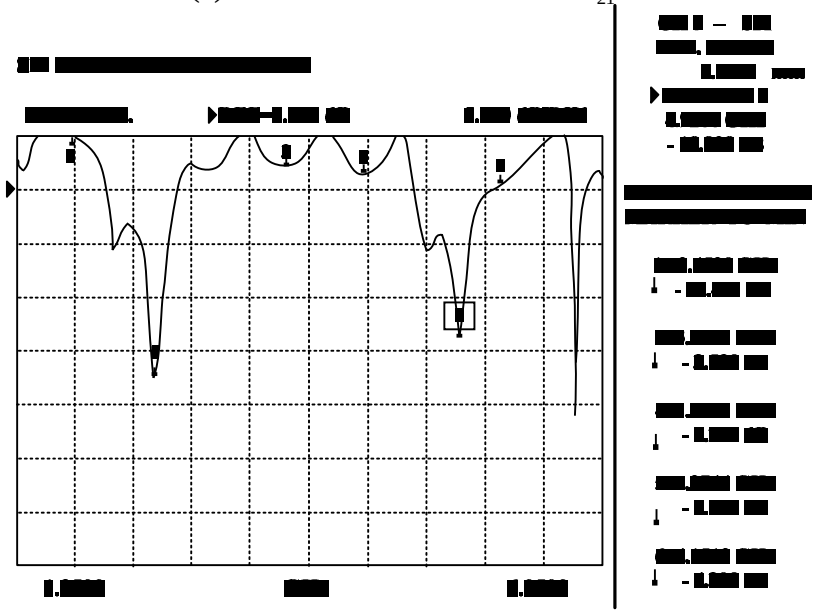

(b) Reflection coefficient S_{11}

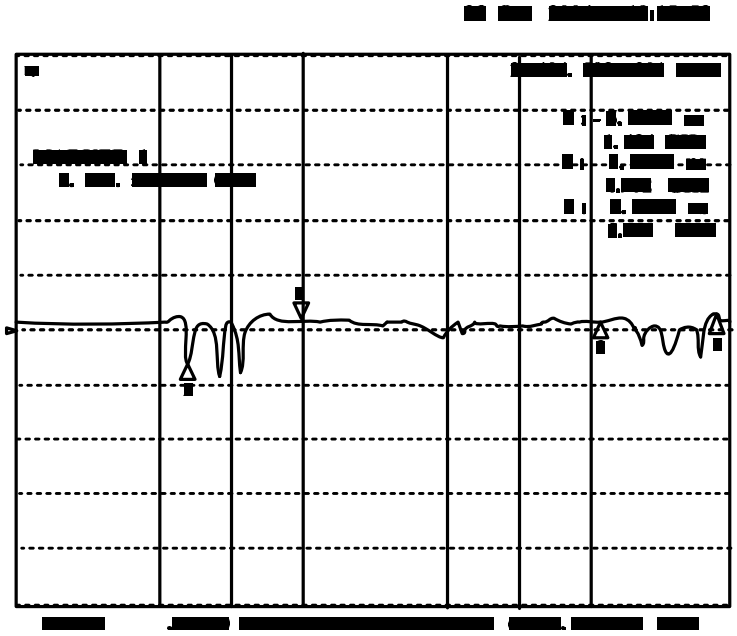

(c) Group Delay

Fig. 4.6 Measurement results: (a) Transmission coefficient. (b) Reflection coefficient. (c) Group Delay

As shown in Fig. 4.6 (a) and (b), there are two pass-bands at each band operation frequency 2.4 GHz and 5.0 GHz. Within these two pass-bands, two optimum transmission coefficients of -0.661 dB and -0.579 dB appear at 2.45 GHz and 4.9 GHz and the reflection coefficients are -22.421 dB and -18.828 dB, relatively. Simultaneously, the measured results show a good suppression characteristic within out-of-bands. There is a little difference with the simulation results resulting from some losses and dissipation by transmission lines and

the experimental precision, but these results are enough to prove that the proposed design method is practical for implementing dual-band pass filters whose dual bands can be controlled based on different demand.

Besides the transmission and the reflection coefficients, there is still an important coefficient left, just group delay. From figure 4.6 (c), the group delays of two pass bands are 1.3914 ns and 1.3752 ns, respectively. They almost agree with the simulation results of 1.2 ns and 1.3 ns shown in figure 4.4 and there are relative flatter characteristics within two pass bands.

CHAPTER 5 Conclusions

This thesis proposes a dual-band pass filter for WLAN (Wireless Local Area Network) 802.11 a/b/g application. There are two pass band centered at 2.4 GHz and 5.0 GHz, respectively. For the sake of implementing this purpose, a wide-band pass filter and a band stop filter are connected directly. The wide-band pass filter is designed by employing ring resonators and the band stop filter is designed by using series-shunted stubs, which all based on microstrip line structure.

The measured results agree well with the simulation results. It is proved that the scheme proposed in this thesis can implement dual-pass-band for WLAN 802.11a/b/g application. By this thesis, we also find that this design method for dual-band is not only used for 802.11a/b/g, but also applied for the other case which needs dual-band frequency responses such as GSM and CDMA application. What we need to do, just adjust the impedance value of the band pass and band stop filter. It's a very useful for mobile communication system.

In future, we will try to reduce the circuit size by using the PCB with high dielectric constant and apply this dual-band pass filter to WLAN 802.11 a/b/g system. Based on this design method of direct connection of a BPF and a BSF, we can also design the others dual-band filters for communication systems.

References

[1] Ian Hunter, *Theory and Design of Microwave Filters*, the Institution of Electrical Engineers, the United Kingdom, 2001.

[2] Jia-Sheng, Hong, M. J. Lancaster, *Microstrip Filters for RF/Microwave Applications*, John Wiley & Sons, Inc, New York, 2001.

[3] IEEE STD 802.11b, *IEEE Standard for Wireless LAN Medium Access Control (MAC) and Phisical Layer (PHY) Specification*, 1999.

[4] Stephen V. Sailiga, Ph.D. *"An Introduction to IEEE 802.11 Wireless LANs,"* Radio Frequency Integrated Circuits (RFIC) Symposium, 2000.

[5] IEEE STD 802.11g, *IEEE Standard for Wireless LAN Medium Access Control (MAC) and Phisical Layer (PHY) Specification*, 1999.

[6] IEEE STD 802.11a, *IEEE Standard for Wireless LAN Medium Access Control (MAC) and Phisical Layer (PHY) Specification*, 1999.

[7] Lin-Chuan Tsai and Ching-Wen Hsue, *"Dual-Band Bandpass Filters Using Equal length Coupled-Serial-Shunted Lines and Z-Transform Technique,"* IEEE Transactions on microwave theory and techniques, Vol. 52, No. 4, pp. 1111-1117, April 2004.

[8] Pozar, David M., *Microwave engineering*, Addison-Wesley, 1990.

[9] J. Helszajn, *Passive and active Microwave Circuits*, Heriot-Watt University Edinburgh, United Kingdom, 1979.

[10] Hitoshi Ishida and Kiyomichi Araki, *"Design and Analysis of Band Pass Filter with Ring Resonator,"* Asia-Pacific Microwave Conference, pp. 96-99, 2003.

[11] Lung-Hwa Hsieh, Kai Chang, "*Compact, Low Insertion-Loss, Sharp-Rejection, and Wide-band Microstrip Bandpass Filters*," IEEE MTT, Vol. 51, No. 4, pp. 1241-1246, April 2003.

[12] ArunChandra Kundu, Ikuo Awai, "*Control of Attenuation Pole Frequency of Dual-Mode Microstrip Ring Resonator Bandpass Filter,*" IEEE MTT., Vol. 49, No. 6, pp. 1113-1117, June 2001.

[13] J. A. G. Malherbe, *Microwave Transmission Line Couplers*, Artech House, Inc., 1988.

[14] M. J. D. Powell, "*A method for minimizing a sum of squares of non-linear functions without calculating derivatives*," Computer Journal, Vol. 7, pp. 303-307, 1965.

[15] George Matthaei, Leo Young, E. M. T. Jones, *Microwave Filters, Impedance-Matching Networks, and Coupling Structures*, Norwood, MA: Artech House, 1985.

[16] Randall W. Rhea, *HF Filter Design and Computer Simulation*, Atlanta Noble Pub., 1994.

[17] B.M. Schiffman and G.L.Matthaei, "*Exact design of band-stop microwave filters*," IEEE Trans., MTT-13, pp. 6-15, May 1964.

[18] M.C. Horton and R.J.Menzel, "*General theory and design of optimum quarter wave TEM filters*," IEEE Trans., MTT-13, pp. 316-327, MAY 1965.

Appendix

Powell's method

Main program

```
clear all;

global Z S
%
%       itmax = maximum number of iterations
%       N     = number of design variables
%
itmax = 20;
N = 3; % various
%
%       initial guess for vector of design variables

 z0 = [50 130 25]';

 Z = z0;
%
%       initial set of search directions grouped into a
%       matrix (each column is a search direction). For
%       Powell's method this matrix is the identity matrix
%
H = eye(N);
%
n = N;
%
%       main iteration loop (n minimizations plus minimization
%       along new conjugate direction)
```

```
%
for iter = 1:1:itmax
    iter
    %
    %       perform n unidimensional minimizations
    %
    S_new = zeros(n,1);
    H;
    for k=1:1:n
        k;
        S = H(:,k);
        alpha_star = fminbnd('fun', -0.5,0.5);
        F = fun(alpha_star);
        Z = Z + alpha_star*S;
        S_new = S_new + alpha_star*S;
    end
    %
    %           generate new search direction, and minimize along it
    %
    S = S_new;
    alpha_star = fminbnd('fun', -0.5, 0.5);
    F = fun(alpha_star)
    Z = Z +alpha_star*S
    %
    %     substitute one of the initial directions with the new one
    %
    for ic=1:1:n-1
        H(:,ic) = H(:,ic+1);
    end
    H(:,n) = S_new;
end
```

Sub-program 1: Calculator of s11 and s21.

```
clc;
clear;
syms Z1 Z2 Z3 f

f0=3.7;

Z0=50;

%% Even-mode %%

ZL1=Z1/(j*tan((pi/2)*(f/f0)));

ZL2=2*Z3/(j*tan((pi/2)*(f/f0)));
ZL3=Z2*(ZL2+j*Z2*tan((pi/2)*(f/f0)))/(Z2+j*ZL2*tan( (pi/2)*(f/f0)));

Zine=(ZL1*ZL3)/(ZL1+ZL3);

Se=(Zine-Z0)/(Zine+Z0);

%% Odd-mode %%

Zl1=j*Z1*tan((pi/2)*(f/f0));

Zl2=j*Z2*tan((pi/2)*(f/f0));

Zino=(Zl1*Zl2)/(Zl1+Zl2);

So=(Zino-Z0)/(Zino+Z0);
```

%% Reflection coefficient %%

s11 = (Se+So)/2

s12 = (Se-So)/2;

s21 = (Se-So)/2

s22 = (Se+So)/2;

Sub-program 2: Parity function

```
function    y = fun(alpha)

global Z S

Z1 = Z(1) + alpha*S(1);
Z2 = Z(2) + alpha*S(2);
Z3 = Z(3) + alpha*S(3);

s11=1/2*(-i*Z1/tan(5/37*pi*f)*Z2*(-2*i*Z3/tan(5/37*pi*f)+i*Z2*tan(5/37*
pi*f))/(Z2+2*Z3)/(-i*Z1/tan(5/37*pi*f)+Z2*(-2*i*Z3/tan(5/37*pi*f)+i*Z2*
tan(5/37*pi*f))/(Z2+2*Z3))-50)/(-i*Z1/tan(5/37*pi*f)*Z2*(-2*i*Z3/tan(5/
37*pi*f)+i*Z2*tan(5/37*pi*f))/(Z2+2*Z3)/(-i*Z1/tan(5/37*pi*f)+Z2*(-
2*i*Z3/tan(5/37*pi*f)+i*Z2*tan(5/37*pi*f))/(Z2+2*Z3))+50)+1/2*(-Z1
*tan(5/37*pi*f)^2*Z2/(i*Z1*tan(5/37*pi*f)+i*Z2*tan(5/37*pi*f))-50)/(-
Z1*tan(5/37* pi*f)^2*Z2/(i*Z1*tan(5/37*pi*f)+i*Z2*tan(5/37*pi*f))+50);

s21=1/2*(-i*Z1/tan(5/37*pi*f)*Z2*(-2*i*Z3/tan(5/37*pi*f)+i*Z2*tan(5/37*
pi*f))/(Z2+2*Z3)/(-i*Z1/tan(5/37*pi*f)+Z2*(-2*i*Z3/tan(5/37*pi*f)+i*Z2*
tan(5/37*pi*f))/(Z2+2*Z3))-50)/(-i*Z1/tan(5/37*pi*f)*Z2*(-2*i*Z3/tan(5/
37*pi*f)+i*Z2*tan(5/37*pi*f))/(Z2+2*Z3)/(-i*Z1/tan(5/37*pi*f)+Z2*(-2*I
*Z3/tan(5/37*pi*f)+i*Z2*tan(5/37*pi*f))/(Z2+2*Z3))+50)-1/2*(-Z1*tan(5
/37*pi*f)^2*Z2/(i*Z1*tan(5/37*pi*f)+i*Z2*tan(5/37*pi*f))-50)/(-Z1*tan(5/
37*pi* f)^2*Z2/(i*Z1*tan(5/37*pi*f)+i*Z2*tan(5/37*pi*f))+50);

%     This is the objective function F to be minimized

segma1 = 0;
for f = 1.35:0.1:2.35
        segma1 = segma1 + (abs(s21))^2+(1-abs(s11))^2;
```

```
end

segma2 = 0;
  for f = 2.35:0.01:5.05
        segma2 = segma2 +(1-abs(s21))+(abs(s11));
end

       segma3 = 0;
for f = 5.05:0.1:6.05
        segma3 = segma3 +(abs(s21))^2+(1-abs(s11))^2;
end

y = segma1+segma2+segma3;
```

Acknowledgements

I would like to thank many people who have helped me during the past two years. Without their supports and encouragements, it is impossible for me to finish my thesis.

I am deeply grateful to my advisor, Professor Dong Il Kim. His wide knowledge, strict research attitude and enthusiasm in work deeply impressed me and taught me what a true scientific research should be. I am also thankful to the other Professors of our department for their supports and guidances on this work, who are Professor Hyung Rae Cho, Professor Kyeong-Sik Min, Professor In-ho Kang, Professor Ki Man Kim, Professor Ji Won Jung, Professor Young Yun, and Young-Su Weon who is the director of Pusan Broadcasting (PSB). I would like to thank Miss Min Jee Kim who is the assistant in our department for her much help in my two-year graduate study life.

Certainly, I cannot be thankful enough to our laboratory members for their timely and unselfish help. They not only help me my research work, but also let me enjoy the friendly work environment and they teach me Korean at anytime when I need. So I have many thanks to Mr.Jun-young Son and Mr. Dong-han Choi they are studying doctor courses and my classmates Mr. Seung-jae Shin, Mr. Sang hyun Moon, Mr. Sang-wook Jeong and my juniors in our laboratory Miss Sin-ja Jang, Mr. Jeong-hyun Choi, Mr. Jae-hyun ‚Jeong, Mr. Dae-hun Kim and Jing-zhen Wu from china too.

I would like to appreciate my chinese friends majoring in the other

majors in our university, including Miss Cai-rong Zheng of my girl friend, Mr. Guo-zhu Jin, Miss Xiao-ling Zhang, Yun-jing Zhang, Mr. Yong-nam Park, Yun-feng Choi, etc. Thanks for their love and supports.

Finally, I would like to express my sincere thanks to Professor Wan-hong Kim from Dalian Maritime University of China. Without his recommendation, it is impossible for me to get this study opportunity in Korea.